Superconductor Science and Technology

Influence of self-fields on the flux-flow dynamics in a long Josephson junction

To cite this article: Marek Jaworski 2004 *Supercond. Sci. Technol.* **17** 327

View the article online for updates and enhancements.

You may also like

- Flux-flow dynamics in a long Josephson junction with nonuniform bias current
Marek Jaworski
- Intrinsic anisotropy and pinning anisotropy in nanostructured $YBa_2Cu_3O_7$ from microwave measurements
N Pompeo, A Alimenti, K Torokhtii et al.
- Fe-based superconducting thin films—preparation and tuning of superconducting properties
J Hänisch, K Iida, R Hühne et al.

This content was downloaded from IP address 18.116.164.246 on 05/05/2024 at 20:29

Supercond. Sci. Technol. **17** (2004) 327–332 PII: S0953-2048(04)68326-6

Influence of self-fields on the flux-flow dynamics in a long Josephson junction

Marek Jaworski

Institute of Physics, Polish Academy of Sciences, Al. Lotników 32/46, 02-668 Warszawa, Poland

E-mail: jawor@ifpan.edu.pl

Received 2 September 2003
Published 7 January 2004
Online at stacks.iop.org/SUST/17/327 (DOI: 10.1088/0953-2048/17/3/005)

Abstract
The flux-flow dynamics in a long Josephson junction is studied for the in-line and overlap geometry. A simple analytical model, reported recently for the overlap case, is extended to include asymmetric boundary conditions resulting from the self-field effects. Analytical results are compared with numerical simulations both for the magnetic field patterns within the junction and for the current–voltage (I–V) characteristics. It is shown that, depending on the junction geometry, the self-field distribution may affect considerably the fluxon dynamics and consequently working conditions of the flux-flow oscillator.

1. Introduction

Multifluxon dynamics in a long one-dimensional Josephson junction has recently attracted considerable interest due to possible applications in superconducting mm-wave electronics [1–3]. Particular attention has been paid to a junction operating in the flux-flow (FF) mode, which can be described briefly as unidirectional collective motion of a dense train of fluxons, created continuously at one end of the junction and annihilated at the other.

Beginning in the early 1980s [4], various aspects of the FF mode have been investigated both theoretically and experimentally. At present, FF oscillators show promising performance; however, some important parameters (e.g. radiation linewidth) are still not satisfactory [5–8]. Thus, there is a need for further efforts to optimize the structure and working conditions of Josephson junctions operating in the FF regime.

In recent years, there has been growing interest in non-uniform junctions, in which asymmetry creates unequal conditions for the fluxon propagation. In this context, inhomogeneous driving has been considered [9], as well as various geometrical structures, including exponential [10], semi-circular [11] and quarter-circular junctions [12]. Relatively less attention has been paid to the asymmetry caused by self-fields, closely related to the constant current flow through the junction. Such self-fields are usually neglected; however, depending on the geometry, they may affect considerably the boundary conditions, and consequently fluxon dynamics within the junction.

The aim of the present work is to study the influence of self-fields on the FF mode behaviour in a long Josephson junction. To this end we compare two distinctly different geometrical structures, in-line and overlap, in which the self-fields affect in a different way the formulation of boundary conditions. In the in-line case, the net magnetic field at the junction ends is a superposition of an external magnetic field and a self-field due to a constant current flowing through the junction. On the other hand, in the overlap geometry the self-fields at the junction ends are negligible while the self-fields along the junction enter the formalism indirectly as a constant bias current density γ [13].

To compare both structures we generalize a simple analytical model reported recently [14, 15]. An approximate solution of the perturbed sine-Gordon (sG) equation consists of a dense fluxon train (FF mode) accompanied by two quasi-linear plasma waves propagating in opposite directions with a velocity close to the critical (Swihart) velocity. Superposition of the FF mode and two plasma waves makes it possible to satisfy boundary conditions for arbitrary time t. Having found an approximate analytical solution, we are able to evaluate the current–voltage (I–V) characteristics of the junction.

The paper is organized as follows. In section 2 we formulate the problem, i.e. we introduce the perturbed sG equation, present two geometrical structures (in-line and overlap) and discuss corresponding boundary conditions. An approximate analytical solution for the FF mode is derived in section 3. We also discuss large-amplitude corrections, which are important in the vicinity of the main FF step,

0953-2048/04/030327+06$30.00 © 2004 IOP Publishing Ltd Printed in the UK

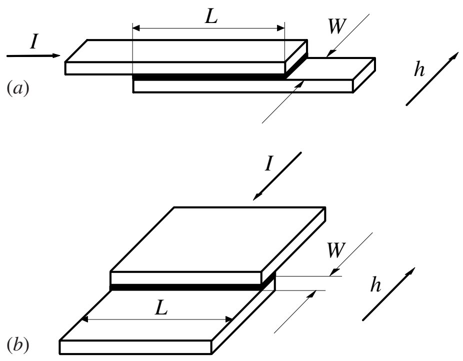

Figure 1. Electrode geometry of a quasi-one-dimensional Josephson junction: (*a*) in-line case; (*b*) overlap case.

where the amplitudes of plasma waves go beyond the quasi-linear limit. In section 4 the *I*–*V* characteristic is derived using a simple perturbation technique. Analytical results are compared with numerical simulations in section 5, both for the instantaneous field patterns within the junction and for the *I*–*V* characteristics. Section 6 contains a summary of the results and concluding remarks.

2. Formulation of the problem

Fluxon dynamics in a long one-dimensional Josephson junction is governed by the perturbed sG equation [13, 16, 17]

$$\phi_{xx} - \phi_{tt} - \alpha\phi_t = \sin\phi - \gamma, \tag{1}$$

where ϕ denotes the quantum phase difference across the junction, α is the loss factor and γ is the normalized bias current density. The space coordinate x has been normalized to the Josephson penetration depth λ_J and time t to the inverse plasma frequency ω_0^{-1}.

Both the current density γ and the boundary conditions at the junction edges depend on the electrode geometry. As mentioned above, in this paper we consider two distinctly different junction structures, shown schematically in figure 1. In quasi-one-dimensional structures we have $W \ll L$, and for a long junction we assume additionally $L \gg 1$.

For the in-line geometry (figure 1(*a*)), the current density γ does not appear explicitly in equation (1), whereas the energy is delivered through the junction ends. Thus, we can set $\gamma = 0$, and assume the boundary conditions [18]

$$\phi_x(-L/2) = h - I/2, \qquad \phi_x(L/2) = h + I/2, \tag{2}$$

where h denotes the normalized external magnetic field and I is the total dc current, generating self-fields at the junction ends.

On the other hand, for the overlap geometry (figure 1(*b*)), the self-fields are negligible at the junction ends and the boundary conditions can be reduced to

$$\phi_x(-L/2) = h, \qquad \phi_x(L/2) = h. \tag{3}$$

The bias current density γ follows from the field distribution in a real two-dimensional junction, and for the overlap geometry can be assumed to be a constant equal to I/L [13].

Thus, we can see that the self-fields play an essential role in the formulation of boundary conditions. As a result, we can expect essentially different solutions of equation (1) for the two geometrical structures outlined above.

3. Approximate analytical solution

In the FF mode, we deal with a unidirectional motion of a fluxon train on a fast rotating background. Following [15, 19, 20] we can write an approximate solution of equation (1) in the form

$$\phi = \phi_0 + \psi, \qquad \psi \ll 1, \tag{4}$$

where ϕ_0 denotes a rotating background term (linearly dependent on time) and ψ is a quasi-linear term representing fluxon motion along the junction.

Substituting equation (4) into the sG equation (1) we obtain for ψ small

$$\phi_{0,xx} + \psi_{xx} - \psi_{tt} - \alpha\Omega - \alpha\psi_t \simeq \sin\phi_0 + \psi\cos\phi_0 - \gamma, \tag{5}$$

where $\Omega = \phi_{0,t}$ denotes the frequency of the background rotation.

In the overlap geometry, the term ϕ_0 was found to be equal to $hx + \Omega t$ [15, 19], thus its x-derivative $\phi_{0,x}$ is constant and equal to the external magnetic field h. In the in-line geometry the boundary conditions (2) imply, however, that the net magnetic field is different at both junction ends, and consequently the term $\phi_{0,x}$ must be x-dependent. Below we consider this case in more detail.

3.1. In-line geometry

To satisfy the boundary conditions (2) we assume a more general form of ϕ_0

$$\phi_0 = \theta(x) + \Omega t, \tag{6}$$

where $\theta(x) = hx + \delta x^2$ and δ is to be determined.

For the in-line geometry we have $\gamma = 0$. Thus, comparing time-independent terms in equation (5) we find

$$\phi_{0,xx} = \alpha\Omega, \tag{7}$$

hence $\delta = \alpha\Omega/2$.

It can be shown [14, 15] that Ω is simultaneously the fundamental frequency of the quasi-linear term ψ. Thus, collecting time-dependent terms in equation (5) we obtain a linear differential equation

$$\psi_{xx} - \psi_{tt} - \alpha\psi_t = \sin\phi_0, \tag{8}$$

where the term $\psi\cos\phi_0$ has been omitted, as giving no contribution of frequency Ω.

To solve equation (8) effectively it is convenient to introduce a complex notation

$$\psi(x,t) = \mathrm{Im}[\tilde{\psi}(x,t)] = \mathrm{Im}[\hat{\psi}(x)\,\mathrm{e}^{\mathrm{i}\Omega t}] \tag{9}$$

and rewrite equation (8) as

$$\hat{\psi}_{xx} + \beta^2\hat{\psi} = \mathrm{e}^{\mathrm{i}\theta}, \tag{10}$$

where $\beta^2 = \Omega^2 - \mathrm{i}\alpha\Omega$.

Using standard methods we find the general solution of equation (10)

$$\hat{\psi} = \frac{\mathrm{e}^{\mathrm{i}\beta x}}{2\mathrm{i}\beta}\int \mathrm{e}^{\mathrm{i}(\theta-\beta x)}\,\mathrm{d}x - \frac{\mathrm{e}^{-\mathrm{i}\beta x}}{2\mathrm{i}\beta}\int \mathrm{e}^{\mathrm{i}(\theta+\beta x)}\,\mathrm{d}x + A\,\mathrm{e}^{\mathrm{i}\beta x} + B\,\mathrm{e}^{-\mathrm{i}\beta x}. \tag{11}$$

The first two terms correspond to a fluxon train propagating unidirectionally along the junction. The last two terms describe plasma waves propagating in opposite directions with a critical velocity $\Omega/\beta \simeq 1$.

For θ being a quadratic function of x, the integrals in equation (11) cannot be calculated analytically. However, we can define

$$F^{\pm}(x) = \int_{-L/2}^{x} \mathrm{e}^{\mathrm{i}(\theta \pm \beta\xi)}\,\mathrm{d}\xi \tag{12}$$

and evaluate the above definite integrals using arbitrary numerical or approximate methods. Note that the lower limit of integration is irrelevant since any constant contribution to those integrals can be incorporated into the constants A and B.

To check the boundary conditions we substitute $\phi = \phi_0 + \psi$ into equation (2). It is clear that the time-independent terms should satisfy

$$\phi_{0,x}(\pm L/2) = h \pm \alpha\Omega L/2 = h \pm I/2, \tag{13}$$

where $I = \alpha\Omega L$ denotes the ohmic line.

The time-dependent term $\psi_x(x,t)$ should vanish at the junction ends, thus for a complex solution we can write

$$\hat{\psi}_x(\pm L/2) = 0. \tag{14}$$

Using equations (11) and (12), and noting that $F^{\pm}(-L/2) = 0$ we find

$$A = \frac{\mathrm{e}^{\mathrm{i}\beta L} F^-(L/2) + F^+(L/2)}{4\beta \sin\beta L}, \qquad B = \frac{F^-(L/2) + \mathrm{e}^{-\mathrm{i}\beta L} F^+(L/2)}{4\beta \sin\beta L}. \tag{15}$$

Substituting the constants A and B into equation (11) and next into equation (4), we obtain finally an approximate analytical solution of equation (1) satisfying the boundary conditions (2) for the in-line geometry. This solution is parametrized by Ω (being proportional to the voltage across the junction) and makes it possible to evaluate the I–V characteristics (see section 4).

3.2. Overlap geometry

For the overlap geometry we neglect the self-fields [13, 18], thus $\theta(x) = hx$ and $\phi_{0,xx} = 0$, which makes further calculations much easier. Comparing time-independent terms we obtain

$$\gamma = I/L = \alpha\Omega, \tag{16}$$

where $I = \alpha\Omega L$ denotes the ohmic line, as before.

For time-dependent terms we obtain a complex solution for $\hat{\psi}(x)$ in the form of equation (11). This time, however, $\theta(x) = hx$ and the solution can be expressed in a fully analytical form:

$$\hat{\psi} = -\frac{\mathrm{e}^{\mathrm{i}hx}}{h^2 - \beta^2} + A\,\mathrm{e}^{\mathrm{i}\beta x} + B\,\mathrm{e}^{-\mathrm{i}\beta x}. \tag{17}$$

As before, the first term corresponds to a fluxon train, while the last two terms describe plasma waves propagating in opposite directions. Imposing the boundary conditions $\hat{\psi}_x(\pm L/2) = 0$ we obtain

$$A = \frac{h \sin[(h+\beta)L/2]}{(h^2 - \beta^2)\beta \sin\beta L}, \qquad B = \frac{h \sin[(h-\beta)L/2]}{(h^2 - \beta^2)\beta \sin\beta L}, \tag{18}$$

where A and B are equivalent to p_1 and p_2, derived in [15, 21].

Substituting A and B into equations (17) and (4) we obtain an approximate analytical solution satisfying boundary conditions (3) for the overlap geometry. However, due to the lack of self-fields at the junction ends, this solution is essentially different from that for the in-line geometry.

3.3. Large-amplitude corrections

So far, we have assumed ψ to be small enough to have

$$\sin\phi \simeq \sin\phi_0 + \psi\cos\phi_0. \tag{19}$$

However, when the amplitudes of the ψ solution are larger, we should use the exact relation

$$\sin\phi = \sin\phi_0 \cos\psi + \sin\psi\cos\phi_0. \tag{20}$$

Note that the real solution ψ can be formally written as

$$\psi(x,t) = \mathrm{Im}[\hat{\psi}(x)\,\mathrm{e}^{\mathrm{i}\Omega t}] = \sum_i (a_i \sin\eta_i + b_i \cos\eta_i), \tag{21}$$

where $\hat{\psi}(x)$ is given in the form of equation (17), a_i and b_i denote real and imaginary parts of complex amplitudes in equation (17), respectively, and η_i is a phase of the ith term.

Substituting equation (21) into equation (20) and using well-known expansions [22] we find the leading time-dependent term to be

$$\sin\phi = P\sin\phi_0 + \ldots, \tag{22}$$

where $P = \prod_i J_0(a_i)J_0(b_i)$ and $J_0(a)$ denotes the Bessel function of the order 0.

If $a_i, b_i \to 0$ then $P \to 1$ and we obtain again the quasi-linear case. However, for a_i, b_i larger, the right-hand side of equation (10) should be multiplied by P defined above. Note that P is dependent on the amplitudes a_i and b_i which are to be determined. Fortunately, the problem can be easily solved iteratively, and for a typical set of parameters only a few steps are required to obtain a self-consistent solution.

It will be shown in section 5 that large-amplitude corrections are relevant only in the overlap case, in which the time-dependent contribution ψ is relatively large in the vicinity of the FF step. In the in-line geometry, however, the amplitude of ψ is much smaller and the quasi-linear approximation (11) yields satisfactory results.

4. Current–voltage characteristics

To evaluate the I–V dependence we consider the Hamiltonian

$$\mathcal{H} = \int_{-L/2}^{L/2} \left[\frac{1}{2}\phi_x^2 + \frac{1}{2}\phi_t^2 + (1 - \cos\phi)\right] \mathrm{d}x \tag{23}$$

and use a simple perturbation procedure based on the energy balance [16, 17].

For a steady-state, strictly periodic solution, the time-averaged change of energy must be equal to zero. Thus, differentiating equation (23) with respect to time and using equation (1) we find the energy balance

$$\int_{-L/2}^{L/2} \left(\gamma \langle \phi_t \rangle - \alpha \langle \phi_t^2 \rangle\right) \mathrm{d}x + \langle \phi_x \phi_t \rangle |_{-L/2}^{L/2} = 0, \qquad (24)$$

where $\langle f(t) \rangle \equiv (1/T) \int_0^T f(t)\,\mathrm{d}t$.

The time derivative ϕ_t of the general solution (4) is given by

$$\phi_t = \phi_{0,t} + \psi_t = \Omega + \Omega\,\mathrm{Re}[\hat{\psi}(x)\,\mathrm{e}^{\mathrm{i}\Omega t}]. \qquad (25)$$

Note that the time-averaged value of ϕ_t is equal to Ω and can be identified with the constant voltage across the junction. On the other hand, $\phi_x(\pm L/2)$ is time-independent and given by appropriate boundary conditions (2) or (3). Hence, the energy balance can be rewritten as

$$\gamma \Omega L - \alpha \int_{-L/2}^{L/2} \langle \phi_t^2 \rangle \,\mathrm{d}x + \Omega \phi_x |_{-L/2}^{L/2} = 0. \qquad (26)$$

For the in-line geometry the bias current density γ is equal to 0 and the energy is delivered through boundaries. According to equations (2) $\phi_x|_{-L/2}^{L/2} = I$, hence

$$I = \frac{\alpha}{\Omega} \int_{-L/2}^{L/2} \langle \phi_t^2 \rangle \,\mathrm{d}x. \qquad (27)$$

For the overlap geometry we have $\gamma = I/L$ but $\phi_x|_{-L/2}^{L/2} = 0$. Hence, substituting these relations into equation (26) we obtain again equation (27). Thus, in spite of different mechanisms of energy supply we obtain the same formula describing the current as a function of ϕ_t, corresponding to a voltage across the junction.

To find the time-averaged value of ϕ_t^2 we note that only quadratic terms contribute, thus using the complex number formalism we find

$$\langle \phi_t^2 \rangle = \Omega^2 \left[1 + \tfrac{1}{2} |\hat{\psi}(x)|^2\right]. \qquad (28)$$

Substituting equation (28) into equation (27) we obtain finally the I–V characteristic

$$I = \alpha \Omega L \left[1 + \frac{1}{2L} \int_{-L/2}^{L/2} |\hat{\psi}(x)|^2 \,\mathrm{d}x\right]. \qquad (29)$$

We can see that the total current I consists of a linear (ohmic) term and a nonlinear contribution following from the Josephson current.

5. Results and discussion

In this section we compare theoretical results derived above with numerical simulations obtained by the finite-difference implicit scheme [23]. An example of the magnetic field distribution within a long junction ($L = 10$) is shown in figure 2 for the in-line geometry. The frequency Ω, i.e. the constant voltage across the junction, has been chosen arbitrarily as $\Omega = 4$, which corresponds to a non-relativistic velocity of the fluxon train. For the remaining parameters we assume realistic values $h = 6$ and $\alpha = 0.1$. The solid line represents an approximate analytical solution of equation (1), given by ϕ_x as a function of x for time t fixed. Open circles show the results of numerical simulations for a discrete set of x values. We can see that the fluxon train is indeed dense; the individual fluxons overlap and their amplitudes are x-dependent, due to the interference with plasma waves.

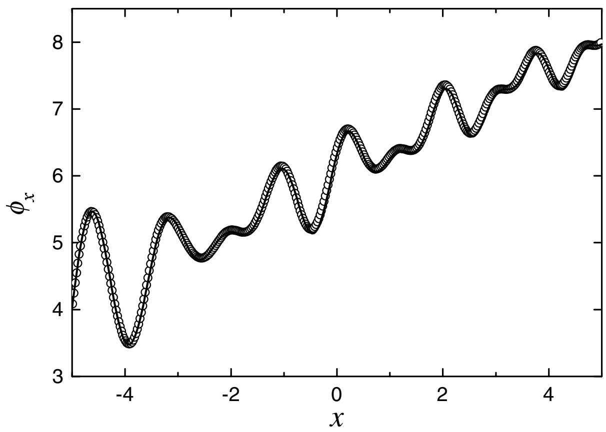

Figure 2. Magnetic field distribution within a long junction in the in-line geometry. An approximate analytical solution (solid line) is compared with numerical results (open circles) for $\Omega = 4$. The remaining parameters are $L = 10$, $h = 6$ and $\alpha = 0.1$.

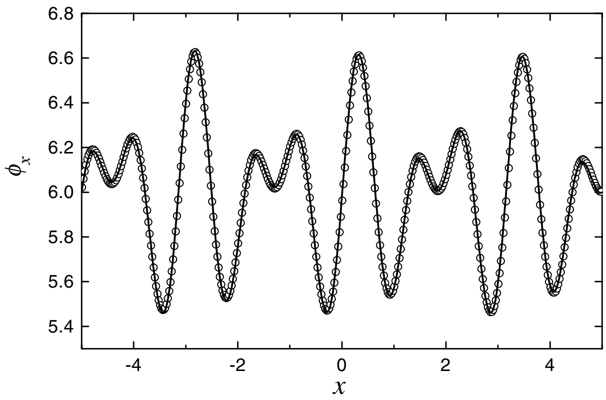

Figure 3. The same as in figure 2 but for the overlap geometry.

According to equation (6), $\phi_{0,x}$ is a linear function of x, making it possible to satisfy boundary conditions (2).

For comparison, figure 3 shows the magnetic field distribution for the same set of parameters but in the overlap geometry. Contrary to the previous case, now $\phi_{0,x}$ is constant and equal to h, while the self-fields enter the formalism indirectly via the constant bias current density γ. As before, fluxons interact with plasma waves, and the resulting amplitude of the fluxon train is x-dependent.

In both structures we can see excellent agreement between analytical and numerical results. This means that the approximate expressions (11) and (17), in spite of their simplicity, reproduce correctly exact solutions of the sG equation (1), subject to appropriate boundary conditions.

The I–V characteristic for the in-line geometry is shown in figures 4(a) and (b). As before, an analytical approximate solution is represented by a solid line, while open circles correspond to numerical results. An analytical approximation follows from equation (29), where Ω has been identified with the constant voltage V across the junction. In the numerical simulations we fix the current I and next evaluate an average value of ϕ_t after sufficiently long evolution (when the solution can be regarded as stationary).

In figure 4(a) we can see a set of equidistant Fiske-like steps on the background of an ohmic line. In the analytical

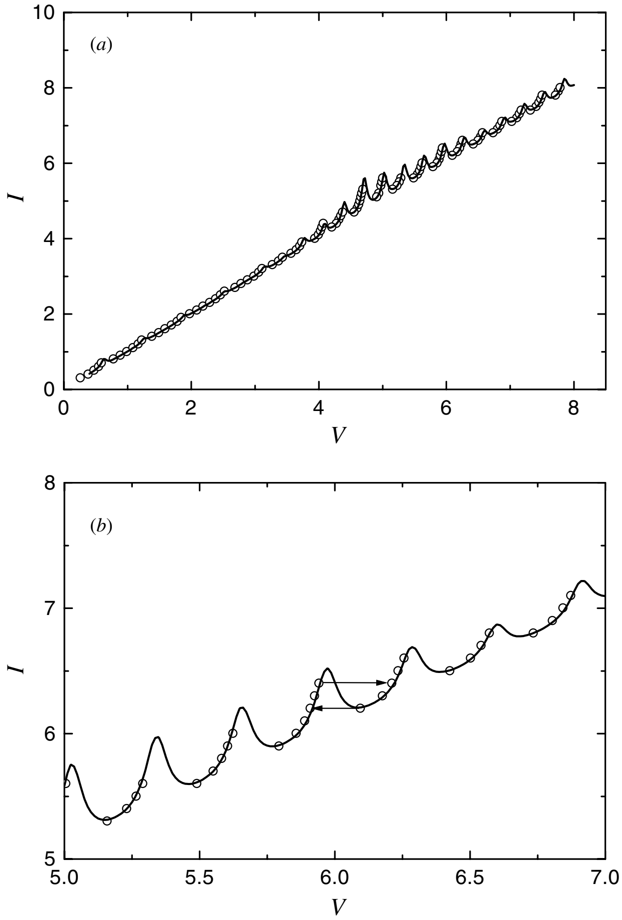

Figure 4. (*a*) *I*–*V* characteristics calculated analytically (solid line) and numerically (open circles) for the in-line geometry. The junction parameters are the same as in figure 2. (*b*) Details of the *I*–*V* characteristics in the vicinity of $V = h$.

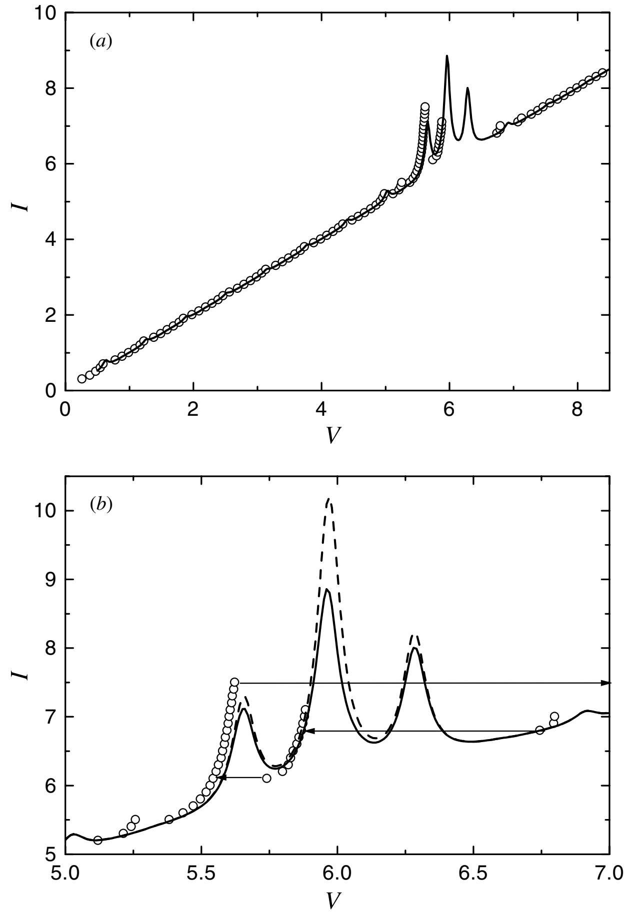

Figure 5. The same as in figure 4 but for the overlap geometry. The dashed line in figure 5(*b*) shows a 'quasi-linear' approximation.

approximation, each step is associated with a segment of negative differential conductivity, which is not visible in the numerical data. On the other hand, numerical results reveal a hysteretic behaviour, as expected. Details of the *I*–*V* curve in the vicinity of $V = h$ are shown in figure 4(*b*).

The *I*–*V* dependence for the overlap geometry (figure 5(*a*)) is essentially different from that of figure 4(*a*). Far from the region $V \simeq h$ we can see basically an ohmic line with small equidistant maxima resulting from the interference with plasma waves. However, in the vicinity of $V = h$, we observe the main FF step accompanied by Fiske-like resonances shifted by π/L from the main peak. Figure 5(*b*) shows details of the *I*–*V* curve in the region $V \simeq h$. Due to relatively large amplitudes of the FF mode and plasma waves appearing in equation (17) for V close to h, we take into account large-amplitude corrections in that region. Additionally, the dashed line shows a 'quasi-linear' approximation (without large-amplitude corrections). It is clear that those corrections are relevant only in the region $V \simeq h$. For other parts of the *I*–*V* dependence as well as for the whole characteristics in the in-line geometry, a quasi-linear approximation is satisfactory.

Similarly as in the in-line case we observe both hysteretic behaviour of numerical solutions and segments of negative conductivity in the analytical expressions. Now, however, strongly nonlinear phenomena are confined to the region ($V \simeq h$). We can argue that the FF step position is strictly dependent on the relation between a constant voltage (V) and a time-independent component of the magnetic field ($\phi_{0,x}$). In other words, a resonance condition responsible for the FF step can be formulated as $V = \phi_{0,x}$.

In the overlap geometry, $\phi_{0,x}$ is a constant equal to h and the FF step is clearly defined. Contrary to this, in the in-line geometry $\phi_{0,x}$ is x-dependent and consequently the resonance condition is satisfied only locally (i.e. at different values of V for different points along the junction). As a result, the main FF step in the *I*–*V* characteristic is so broadened that it practically disappears. Instead, we can see that the amplitudes of Fiske-like steps are generally small and only weakly dependent on the voltage.

6. Concluding remarks

In the present paper we have discussed the influence of self-fields on the FF dynamics in a long Josephson junction. In particular, we have focused on two essentially different structures, in-line and overlap, for which the junction geometry implies the distribution of self-fields and consequently appropriate boundary conditions.

Extending the model outlined in [14, 15], we have derived an approximate analytical solution of the sG equation, consisting of the FF mode associated with two oppositely directed plasma waves. Next, the *I–V* characteristics have been found using a simple perturbation scheme.

The agreement between analytical and numerical results is excellent, which means that a simple approximation presented here is able to reproduce correctly all the relevant features of the solution. On the other hand, the comparison of results obtained for in-line and overlap structures indicates important differences in the FF dynamics. In particular, it turns out that the relation between a constant voltage (V) and a constant (time-independent) magnetic field ($\phi_{0,x}$) within the junction is crucial for the main FF step behaviour in the *I–V* characteristic.

In the overlap geometry, the (time-averaged) magnetic field is independent of x and equal to h, which implies that the main step is well defined at $V = h$. On the other hand, in the in-line case, the time-averaged magnetic field is a function of x. As a result, the main step is spread over the whole voltage range and cannot be detected in the *I–V* characteristic.

It is known [7, 8] that the *I–V* dependence in the vicinity of the main FF step is responsible for some practically important parameters of the FF oscillator (such as linewidth). In this context, the overlap geometry, exhibiting large segment of negative differential conductivity, seems to be superior to other structures. In general, however, the self-fields play an important role in the fluxon dynamics and cannot be neglected in the analysis of FF phenomena in long Josephson junctions.

Finally, it should be noted that the formalism presented here is not restricted to the analysis of self-field effects. From the formal point of view, the method is applicable to arbitrary asymmetric boundary conditions (not only those related to the in-line geometry). Thus, the approximate solution derived in the present paper may be useful in the analysis of other asymmetric structures, such as a Josephson junction immersed in a non-uniform external magnetic field.

Acknowledgment

This work was supported by the KBN Grant No. 2P03B 097 22.

References

[1] Koshelets V P, Shchukin A V, Shitov S V and Filippenko L V 1993 *IEEE Trans. Appl. Supercond.* **3** 2524
[2] Mygind J, Koshelets V P, Shchukin A V, Shitov S V and Lapytskaya I L 1995 *IEEE Trans. Appl. Supercond.* **5** 2951
[3] Koshelets V P and Shitov S V 2000 *Supercond. Sci. Technol.* **13** R53
[4] Nagatsuma T, Enpuku K, Irie F and Yoshida K 1983 *J. Appl. Phys.* **54** 3302
Nagatsuma T, Enpuku K, Yoshida K and Irie F 1984 *J. Appl. Phys.* **56** 3284
Nagatsuma T, Enpuku K, Sueoka K, Yoshida K and Irie F 1985 *J. Appl. Phys.* **58** 441
Qin J, Enpuku K and Yoshida K 1988 *J. Appl. Phys.* **63** 1130
[5] Koshelets V P, Shchukin A, Lapytskaya I L and Mygind J 1995 *Phys. Rev.* B **51** 6536
[6] Ustinov A V, Kohlstedt H and Henne P 1996 *Phys. Rev. Lett.* **77** 3617
[7] Salerno M, Samuelsen M R and Yulin A V 2001 *Phys. Rev. Lett.* **86** 5397
[8] Pankratov A L 2002 *Phys. Rev.* B **65** 054504
[9] Pankratov A L 2002 *Phys. Rev.* B **66** 134526
[10] Carapella G, Martuciello N and Costabile G 2002 *Phys. Rev.* B **66** 134531
[11] Shaju P D and Kuriakose V C 2002 *Phys. Rev.* B **65** 214508
[12] Shaju P D and Kuriakose V C 2003 *Supercond. Sci. Technol.* **16** L25
[13] Lomdahl P S 1985 *J. Stat. Phys.* **39** 551
[14] Jaworski M 1998 *Phys. Lett.* A **244** 97
[15] Jaworski M 1999 *Phys. Rev.* B **60** 7484
[16] McLaughlin D W and Scott A C 1978 *Phys. Rev.* A **18** 1652
[17] Kivshar Y S and Malomed B A 1989 *Rev. Mod. Phys.* **61** 763
[18] Barone A and Paterno G 1982 *Physics and Applications of the Josephson Effect* (New York: Wiley)
[19] Cirillo M, Grønbech-Jensen N, Samuelsen M R, Salerno M and Verona Rinati G 1998 *Phys. Rev.* B **58** 12377
[20] Salerno M and Samuelsen M R 1999 *Phys. Rev.* B **59** 14653
[21] Jaworski M 2001 *Phys. Rev.* B **63** 104504
[22] Abramowitz M and Stegun I A 1982 *Handbook of Mathematical Functions* (New York: Dover)
[23] Dodd R K, Eilbeck J C, Gibbon J D and Morris H C 1982 *Solitons and Nonlinear Wave Equations* (London: Academic)